*Composites Science and Technology* **48** (1993) 161–172

# CONTINUOUS-GLASS-FIBRE-REINFORCED POLYPROPYLENE COMPOSITES: I. INFLUENCE OF MALEIC-ANHYDRIDE-MODIFIED POLYPROPYLENE ON MECHANICAL PROPERTIES

H. A. Rijsdijk, M. Contant & A. A. J. M. Peijs*

*Centre for Polymers and Composites, Eindhoven University of Technology, P.O. Box 513, 5600 MB Eindhoven, Netherlands*

(Received 29 June 1992; revised version received 3 September 1992; accepted 23 November 1992)

**Abstract**

*This study investigates the influence of maleic-anhydride-modified polypropylene (m-PP) on monotonic mechanical properties of continuous-glass-fibre-reinforced polypropylene (PP) composites. Maleic-anhydride-modified polypropylene was added to the PP homopolymer to improve the adhesion between the matrix and the glass fibre. Three-point bending tests were performed on 0° and 90° unidirectional glass-fibre/PP laminates with various weight fractions of m-PP in the PP matrix. These tests showed an increase in both longitudinal and transverse flexural strength up to 10 wt% m-PP, whereas at higher weight fractions of m-PP a decrease in flexural strength was observed. No significant influence of m-PP on composite stiffness was observed. Additional mechanical tests on unidirectional glass/PP composites with 0 wt% and 10 wt% m-PP showed only a small increase in fibre-dominated properties such as longitudinal tensile strength and strain, whereas composite properties that are governed by the interphase, such as transverse, shear and compressive strength, showed significant increases as a result of matrix modification and an enhanced interaction between the glass fibres and the PP matrix.*

*Keywords:* polymer matrix composite, glass fibre, polypropylene, adhesion, fibre/matrix interface, chemically modified polypropylene, mechanical properties

## 1 INTRODUCTION

The development of thermoplastic resins as matrices for continuous-fibre-reinforced composites has offered considerable advantages over thermoset polymers in composite structures with regard to processing, handling, damage tolerance, environmental resistance and recycling. Since the mid-1980s a considerable amount of research has been devoted to the use of thermoplastic composites.[1,2] However, most research activities have been limited to composites based on high-performance speciality resins such as poly(ether ether ketone) (PEEK), poly(ether sulphone) (PES) and poly(ether mide) (PEI), with prices which in some cases even exceed those of carbon fibres. The material APC-2, based on carbon-fibre/PEEK, has particularly been very well documented.[3] However, applications of these high-price, high-performance composite systems are limited to relatively small markets such as aerospace applications.

The cost-effectiveness of a structure depends not only on performance or manufacturing costs, but also on raw material costs. Consequently, the economic potential of continuous-fibre-reinforced composites based on glass fibres and commodity plastics such as poly(ethylene terephthalate) (PET), polyamide (PA) and polypropylene (PP), in combination with the potential advantage of high production rates, may attract large-volume markets such as the automotive industries.

Nowadays, thermoplastic 'bulk' composites have two established technologies: first, short-fibre-reinforced injection moulding compounds and second, glass mat thermoplastics (GMTs), i.e. stampable sheet products based on moderate loadings of relatively long fibres in random array.[4] Recently, there have been some developments in the field of continuous-glass-fibre-reinforced composites based on commodity thermoplastics[5,6] to fill the gap between high-performance composite systems such as PEEK/carbon APC-2 and GMTs with relatively limited performance. Such materials, together with the technology, are now becoming available, and offer the designer the opportunity to incorporate high load-bearing capability into structures manufactured in high-rate processes.

To be successful in replacing traditional materials

* To whom all correspondence should be addressed.

*Composites Science and Technology* 0266-3538/93/$06.00

such as steel, a material has to be cost-effective over its lifetime. This means that the performance of a material has to be considered on the basis of its lifetime. An important aspect with respect to the use of semi-crystalline thermoplastic composites is the possibility of affecting the matrix morphology by processing conditions. Consequently, most studies directed towards optimizing the performance of thermoplastic composites based on crystalline polymers have focused on the effect of processing conditions such as cooling rates on matrix morphology and mechanical properties.[3,7,8] Another important aspect in the performance and durability of fibre-reinforced thermoplastics is the adhesion between the fibre and the matrix. It is generally recognized that the mechanical properties of fibre-reinforced materials are strongly dependent on the quality of the fibre/matrix interface. As poor adhesion usually results in poor composite properties, there is a growing interest in composite research focusing on interfacial phenomena and their effect on composite performance.[9,10] Experimental studies on carbon fibre/epoxy composites[11–14] showed that shear, transverse and compressive properties were strongly dominated by the adhesion between the matrix and the fibre. In addition to monotonic (off-axis) properties such as shear and transverse properties, the fracture toughness[11,15] and long-term properties such as fatigue[16,17] are also strongly dependent on the interaction between matrix and fibre.

The interaction between the matrix and the fibre can be improved by using a fibre with a sizing specific to the polymer matrix. In the case of glass fibres, organofunctional silanes may be used as adhesion promoters between the organic matrix and the glass fibre. The function of sizing agents and their interaction and reaction with fibres and polymers have been reviewed by Ishida[18] and Plueddemann.[19] Apolar polymers such as polypropylene (PP) and polyethylene (PE) have limited interaction with a sizing specific for these polymers. To resolve this problem, the PP should be modified to increase the interaction between the matrix and the sized fibre. Pull-out experiments by Mäder and Freitag[20] showed that the bond strength in a PP/glass system was dependent on the modification of the PP matrix rather than on the type of sizing. Fibre/matrix systems that can be used to achieve optimum adhesion between the fibres and the matrix include acrylic-acid-grafted PP and maleic-anhydride-modified PP in combination with glass fibre with compatible sizings. Such a sizing, containing amide groups, can increase the interaction between the PP matrix and the glass fibre by chemical reaction.[21] Studies on the influence of acrylic-acid-grafted PP on the mechanical properties of short-glass-fibre-reinforced polypropylene compounds showed that the performance of such materials can be improved by addition of chemically modified PP.[22,23] Recently, the development of such chemically modified PPs resulted in the introduction of a second-generation GMT sheet with better adhesion between the fibres and the matrix.

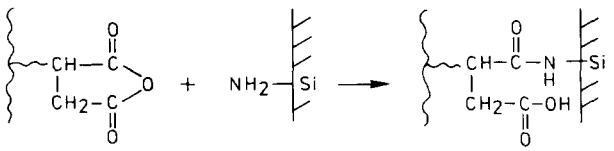

This paper contains the first part of a series of papers on the optimization and characterization of mechanical properties of unidirectional-glass-fibre-reinforced PP composites, including the effect of the interface on these properties. This paper deals with the influence of maleic-anhydride-modified polypropylene (m-PP) on the mechanical properties of continuous-glass-fibre-reinforced PP composites. Additional papers will deal with the effect of m-PP on fracture toughness and long-term properties such as fatigue.

## 2 EXPERIMENTAL

### 2.1 Materials

Unidirectional laminates of 250 mm × 300 mm were manufactured by a film stacking method, where fibres are wound on a rectangular mandrel with alternating layers of polymer films (Fig. 1). After film stacking, the mandrel with layers of polymer and glass fibres was placed in an oven for 60 min at 90°C for drying. A typical laminate with a thickness of 2 mm consisted of approximately 10 layers of fibres with alternating layers of polymer film.

Subsequently, the mandrel was placed between two release coated Mylar® sheets and two steel plates. Metal stop-strips were used to control the thickness of the laminate. The material was melted at 200°C and pressed for 45 min at 25 bar. After hot-pressing, the composite was slowly cooled in the hot-press. Despite the problems of wetting the fibres in a film stacking process, this manufacturing technique was chosen as it is convenient for the preparation of small quantities of composites. An additional benefit of this technology is that it is based on flat film, a product form that is easily prepared in our laboratory in various compositions using film-blowing equipment.

In this study we used a continuous glass fibre from PPG Industries Fiber Glass BV (PPG 854-6-S28-1200) and a PP matrix (homopolymer VM6100, melt flow index 20) from Shell Chemicals. To increase the interfacial bond strength between the glass fibre and the PP matrix, a maleic-anhydride-modified PP from BP Chemicals (Polybond 3002) was added to the PP matrix.

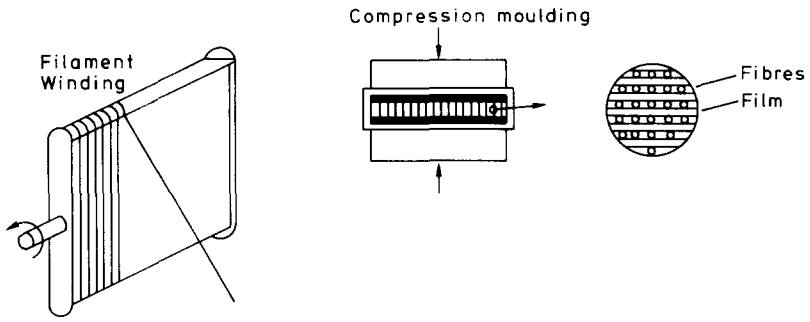


**Fig. 1.** Manufacture of unidirectional laminates by film stacking method.

### 2.2 Test specimens

Test specimens were cut from the unidirectional composite plates. To remove cutting irregularities, specimen edges were subjected to several grinding operations. Aluminium end-tabs were adhesively bonded to the tensile and compression specimens. The specimen dimensions for tensile, compression and bending tests are summarized in Table 1. The fibre volume fraction of all unidirectional specimens was 0·58, with a standard deviation of 0·02. All tested laminates showed good wetting of the fibres by the polymer matrix. A minimum of five specimens were tested for each case.

### 2.3 Testing

*2.3.1 Flexural testing*

Three-point bending tests were performed according to ASTM D-790 on a Frank tensile machine, type 81565. The span-to-depth ratio of the specimens was 40, using a span of 80 mm. The test speed was 5 mm $min^{-1}$. Flexural strength was calculated from the maximum force at failure using the equation

$$\sigma_{max} = \frac{3}{2}\frac{F_{max}L}{wt^2}\left[1 + 6\left(\frac{D}{L}\right)^2 - 4\left(\frac{t}{L}\right)\left(\frac{D}{L}\right)\right] \quad (1)$$

where $\sigma_{max}$ is the failure stress, $F_{max}$ is the force at failure, $L$ is the span, and $w$ and $t$ are the width and thickness of the specimen, respectively. The mid-point deflection $D$ was determined from the crosshead displacement. An approximate correction factor is given in eqn (1) to correct for the end forces in the beams as a result of relatively large deflections in beams of large support span-to-depth ratio. The Young's modulus can be calculated with the relationship

$$E = \frac{L^3}{4wt^3}\frac{F}{Y} \quad (2)$$

where $Y$ is the displacement of the traverse. The strain to failure is determined by

$$\varepsilon_{max} = \frac{\sigma_{max}}{E} = \frac{6t}{L^2}Y_{max} \quad (3)$$

where $Y_{max}$ is the displacement of the traverse at failure. The weight fraction m-PP in the PP matrix of the specimens was varied between 0 wt% and 100 wt%. Fracture surfaces of the various 0° and 90° test specimens were investigated by scanning electron microscopy (SEM) (Cambridge Stereoscan S200) to illustrate differences in failure modes.

Upon loading, damage occurs, and the energy released results in the generation of shock waves in the composite material. By using acoustic emission (AE) methods these shock waves can be detected with a piezo-electrical sensor placed on the surface of the specimen. During flexural testing of 0° and 90° specimens, damage initiation and development was real-time monitored with an acoustic emission system (PAC 8900 Locan AT) from Physical Acoustics Corp., including a 40 dB preamplifier (PAC 1200A). Acoustic emission was detected with a piezo-electrical transducer (PACR15) placed on the end of the specimen with vacuum grease. A threshold of 25 dB was used to reduce background noise. As the intake of AE signals is limited to a certain number of events per second, in the case of the longitudinal bending tests, a low crosshead speed of 1·5 mm $min^{-1}$ was used.

*2.3.2 Tensile testing*

Longitudinal tensile tests were performed on a Zwick universal testing machine (type 1484) at a crosshead

**Table 1. Specimen dimensions**

| Test | Thickness (mm) | Width (mm) | Length between tabs (mm) |
|---|---|---|---|
| *Bending* | | | |
| [0] | 2·0 | 12 | — |
| [90] | 2·0 | 25 | — |
| SBS | 3·0 | 10 | — |
| *Tension* | | | |
| [0] | 2·0 | 12 | 160 |
| [10] | 2·0 | 12 | 160 |
| [±45] | 2·4 | 15 | 100 |
| [90] | 2·0 | 25 | 60 |
| *Compression* | | | |
| [0] | 4·5 | 20 | 15 |
| [90] | 4·5 | 20 | 15 |

speed of 1 mm $min^{-1}$. The longitudinal tensile strain was monitored by means of an extensiometer. Transverse tensile tests were carried out on a Frank tensile machine (type 81565). The crosshead speed used for transverse tensile tests was 0·5 mm $min^{-1}$. The transverse tensile strain was determined from the traverse displacement.

*2.3.3 Shear testing*

The in-plane shear strength, $\tau_{12}$, was determined from two types of shear tests, i.e. 10° off-axis and ±45° tensile tests, at a crosshead speed of 1 mm $min^{-1}$. For the 10° off-axis test the shear strength was determined from the maximum applied stress, $\sigma_x$, at an angle $\theta$, by using

$$\tau_{12} = -\sigma_x \cos\theta \sin\theta \quad (4)$$

The shear strength for a uniaxial test on a ±45 laminate is given by

$$\tau_{12} = \frac{\sigma_x}{2} \quad (5)$$

The interlaminar shear strength (ILSS) was determined using the short beam shear (SBS) test. Tests were performed according to ASTM D-2344 specifications on unidirectional composites using a span-to-depth ratio of four and a test speed of 1 mm $min^{-1}$.

*2.3.4 Compression testing*

Compression tests were performed on a Zwick universal testing machine (type 1484), at a crosshead speed of 0·5 mm $min^{-1}$. Test specimens were in accordance with ASTM D-3410, with the exception that the Celanese type of test fixture used in this study also allowed for specimen widths other than the standard 6 mm (Fig. 2).

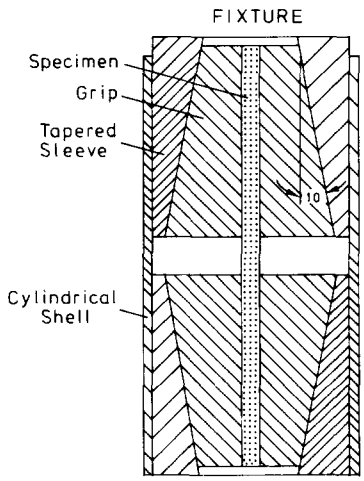


**Fig. 2.** Test fixture used for compression tests.

## 3 RESULTS AND DISCUSSION

### 3.1 Optimization of composite system

*3.1.1 Fibre impregnation*

Long-term properties of polymer composites such as creep and fatigue are dependent on the molecular weight of the matrix,[24] especially when these properties are dominated by the matrix. High molecular weight, which is associated with a low melt flow index (MFI), usually implies better long-term behaviour. On the other hand, low MFIs mean high viscosities, which might cause problems in fully wetting the fibres in melt impregnation processes such as film stacking. As poor impregnation usually results in poor stress transfer from the matrix to the fibre and consequently also poor composite properties,[25] consolidation in film stacking processes often involves applying high pressures for long periods of time.[26]

To optimize the composite material with respect to a uniform fibre distribution, an initial study was undertaken to investigate the influence of processing conditions such as pressure, time and resin viscosity on the impregnation of fibres. Figure 3(a)–(c) compares cross-sectional micrographs of composites with three PPs (MFI = 3, 10 and 20) after pressing for 45 min at 25 bar and 200°C. These micrographs show that an increase in MFI results in better wetting of the glass fibres. In the case of a PP matrix with an MFI of 20 the glass fibres were all well encapsulated by the matrix (Fig. 3(c)). However, MFIs lower than 10 (Fig. 3(a)) lead to poor impregnation of glass fibres.

Based on these experiments, a PP with an MFI of 20 was chosen as the principal matrix in this experimental study. However, care should be taken with respect to the definition of an 'optimum' composite microstructure, as less desirable fibre/matrix distributions with resin-rich interlayers such as shown in Fig. 3(a) might result in improved interlaminar toughness of polymer composites. In fact, the development of interleaved composites is based on the incorporation of such tough resin-rich interply layers.[27]

*3.1.2 Fibre/matrix adhesion*

The longitudinal and transverse flexural properties of unidirectional glass/PP composites are summarized in Table 2 for various weight fractions of m.PP in the PP matrix. Also included in this table are the mechanical properties of the pure polymer matrix as determined by tensile testing of specimens with various compositions.

*3.1.2.1 Transverse flexural properties.* Figure 4 shows the stress/strain curves of the transversely loaded glass/PP composites. Approximate linear elastic behaviour up to fracture of the composite was observed for all specimens. The cumulative plots of events vs time for all types of glass/PP composites are

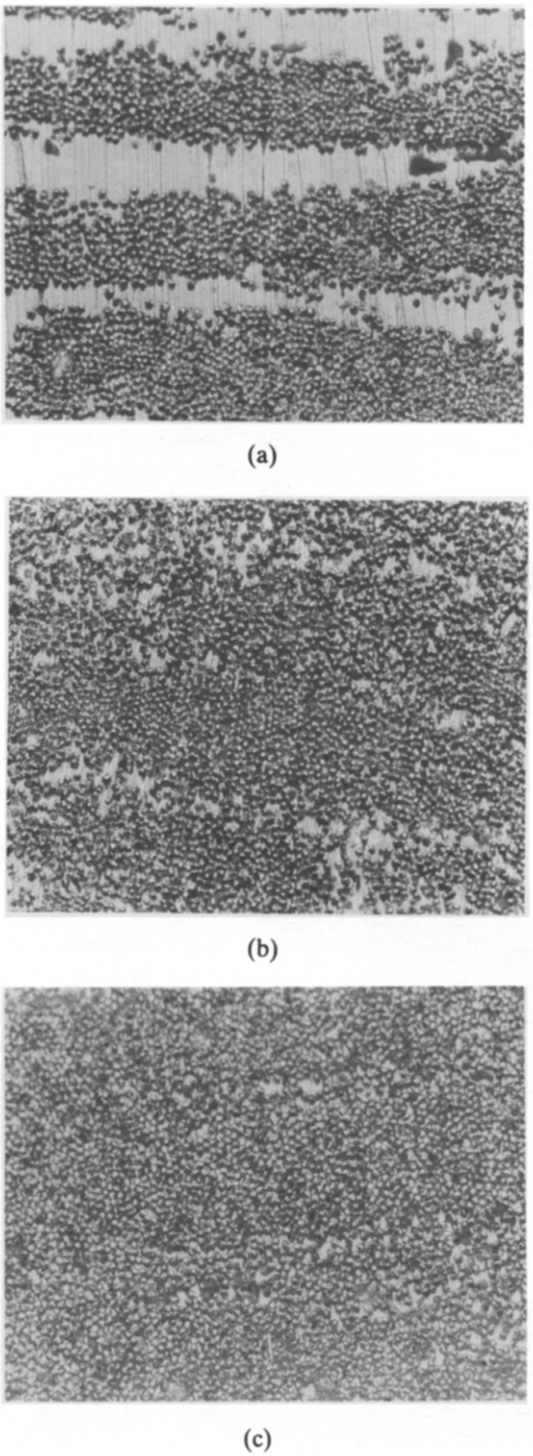


**Fig. 3.** Cross-sections of PP/glass composites: (a) MFI = 3, showing no impregnation; (b) MFI = 10, showing poor impregnation; (c) MFI = 20, showing good impregnation.

shown in Fig. 5. The increase in strain to failure (Table 2) also resulted in an increase in the onset of damage for composites based on a matrix with 10 wt% m-PP. Composites with 10 wt% m-PP showed a rapid increase in emissions at approximately 65% of the maximum load, whereas composites with 0 wt% m-PP showed an onset of damage at approximately 30% of the maximum load.

A comparison of the transverse flexural strengths of the glass fibre/PP composites with various weight fractions of m-PP is shown in Fig. 6. The transverse flexural strength increased up to 10 wt% m-PP, whereas at higher weight fractions of m-PP a decrease in transverse strength was observed. Scanning electron micrographs of the fracture surfaces of failed specimens (Fig. 7(a)–(c)) showed a change in failure mode from interface failure for composites with 0 wt% m-PP to matrix fracture for composites based on a 10 wt% m-PP matrix, whereas at 100 wt% m-PP interface failure was again observed (Fig. 7(c)). However, some evidence of thin layers of matrix material on the surface of the glass fibre suggested that, in addition to interface failure, matrix or 'interphase' failure also occurred. The typical case of matrix fracture for composites with 10 wt% m-PP and a transverse composite strength close to that of the pure resin indicated that an optimum in interaction between the matrix and the fibre was reached and that composite properties for this system are matrix dominated rather than interface dominated. Consequently, a further increase in the amount of m-PP will not result in a further increase in fibre/matrix bond strength. However, this would also imply a constant transverse strength rather than a decrease if we assume that the amount of m-PP has no influence on the matrix or interphase properties. Because, at higher (>10 wt%) weight fractions m-PP, a decrease in transverse strength was observed, addition of m-PP also seems to cause deterioration in the matrix and/or interphase properties and consequently in the transverse properties of the composites.

Experiments on unreinforced polymers showed no negative effects of the addition of m-PP on the tensile strength of m-PP/PP blends. However, as the morphology and consequently the properties of a crystalline polymer such as PP are influenced by the presence of glass fibres,[30,31] it is difficult to relate unreinforced resin properties as listed in Table 2 to the properties of the polymer matrix in a real composite.

In general, the transverse flexural modulus of the composites (Fig. 8) was not significantly influenced by the amount of m-PP, except for the flexural modulus of the glass/PP composite with 0 wt% m-PP. This effect might be caused by interfacial changes, such as the formation of a more brittle interphase, as a result of the addition of m-PP. However, as the deviation in moduli is rather high, care should be taken in drawing conclusions from these data.

To study in more detail the effect of m-PP on the interphase composition and morphology, surface analytical techniques such as Fourier transform IR (FTIR) and secondary ion mass spectroscopy (SIMS)

**Table 2. Flexural properties of the glass/PP composites and tensile properties of the PP matrix at various weight fractions of m-PP in the PP matrix**

| | m-PP (wt%) | | | | | | |
|---|---|---|---|---|---|---|---|
| | 0 | 5 | 10 | 20 | 40 | 60 | 100 |
| *Composite* | | | | | | | |
| $\sigma_{trans}$ (MPa) | 8·6 | 14·6 | 20·6 | 10·6 | 12·7 | 15·0 | 14·8 |
| $\sigma_{long}$ (MPa) | 774 | 806 | 1037 | 720 | 620 | 800 | 740 |
| $E_{trans}$ (GPa) | 4·9 | 6·0 | 6·8 | 5·4 | 5·8 | 6·8 | 6·4 |
| $E_{long}$ (GPa) | 38·5 | 36·5 | 32·0 | 33·6 | 35·8 | 31·8 | 32·6 |
| $\varepsilon_{trans}$ (%) | 0·15 | 0·24 | 0·31 | 0·23 | 0·22 | 0·24 | 0·23 |
| $\varepsilon_{long}$ (%) | 2·11 | 2·31 | 3·34 | 2·24 | 1·83 | 2·60 | 2·37 |
| *Matrix*[a] | | | | | | | |
| $\sigma$ (MPa) | 27·5 | 29·0 | 29·4 | 29·2 | 28·8 | 33·2 | 32·3 |
| $E$ (GPa) | 1·5 | 1·5 | 1·7 | 1·5 | 1·7 | 1·5 | 1·6 |
| $\varepsilon$ (%) | 5·3 | 5·0 | 5·1 | 5·6 | 4·0 | 9·7 | 9·8 |

[a] The matrix specimens were manufactured under the same conditions as the composite specimens. Under these conditions, i.e. low cooling rate and high pressure, the PP will be rather elastic.[28,29]

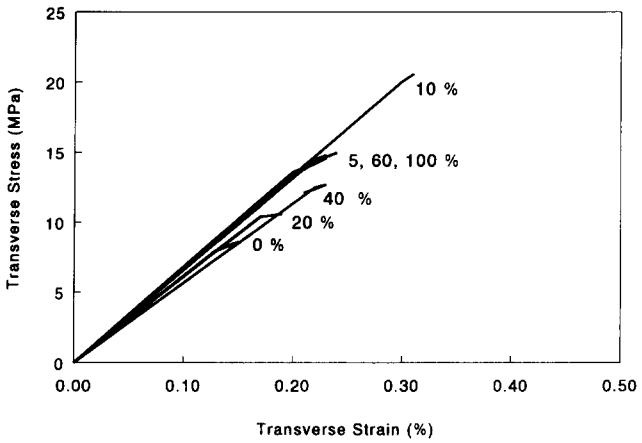


**Fig. 4.** Transverse stress/strain curves of glass/PP composites.

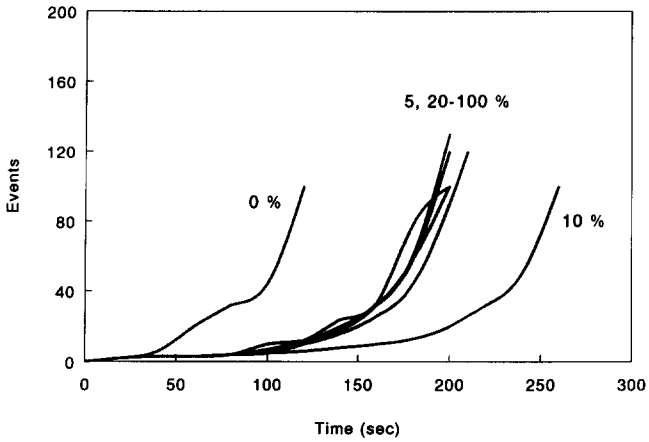


**Fig. 5.** Cumulative AE plots of transversely loaded glass/PP composites.

will be used on model composites of sized glass slides with thin films of PP/m-PP blends. Results of this study will be published in a forthcoming paper.

*3.1.2.2 Longitudinal flexural properties.* The stress/strain curves of the unidirectional glass/PP composites after three-point bend testing of longitudinal specimens with various weight fractions of m-PP in the PP matrix are shown in Fig. 9. Linear elastic behaviour up to fracture of the composite was observed for all specimens.

The cumulative plots of acoustic events vs time for all composites are shown in Fig. 10. A trend in AE signals for longitudinal bending experiments similar to that found by transverse testing (Fig. 5) is observed. Also, similar to the failure strain differences between

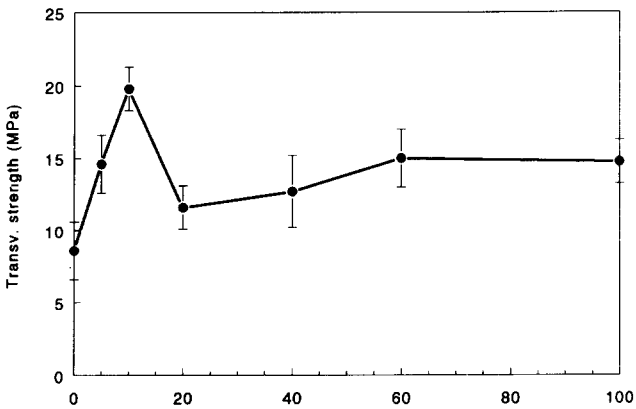


**Fig. 6.** Transverse flexural strength of glass/PP composites as a function of the weight fraction of m-PP in the PP matrix.

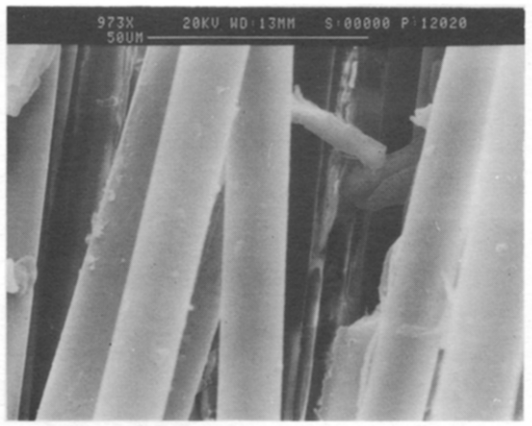


(a)

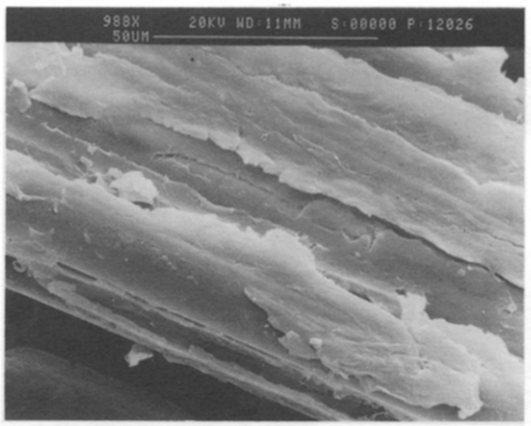


(b)

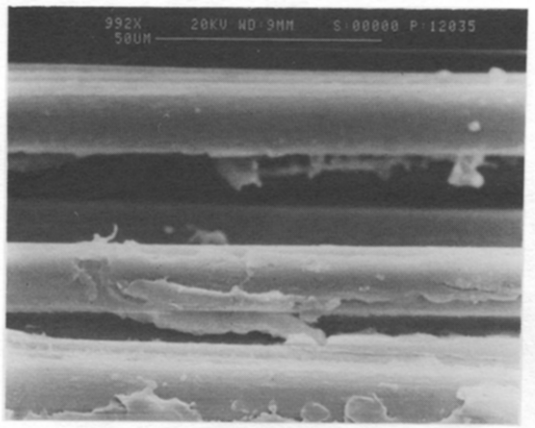


(c)

**Fig. 7.** Scanning electron micrographs of transverse fracture surfaces showing (a) interface failure at 0 wt% m-PP, (b) matrix failure at 10 wt% m-PP and (c) a combination of interface and matrix failure at 100 wt% m-PP.

the various composites (Table 2), the onset of damage shifted to larger time periods. A sharp increase in event rate was observed at approximately 40% and 60% of the maximum load for the 0 wt% and 10 wt% m-PP composites, respectively.

Amplitude distribution analysis of AE signals has been shown to be useful in discriminating between fracture mechanisms in fibre-reinforced materials.[17,32]

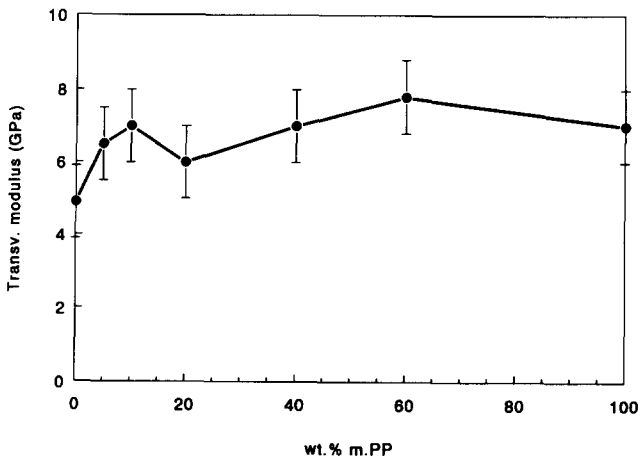


**Fig. 8.** Transverse flexural modulus of the glass/PP composites as a function of the weight fraction of m-PP in the PP matrix.

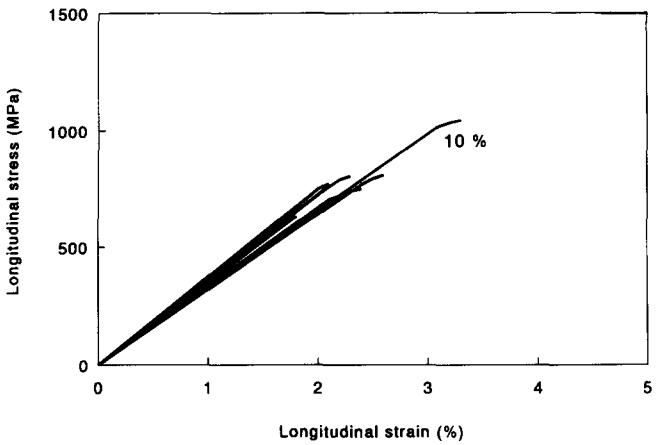


**Fig. 9.** Longitudinal stress/strain curves of glass/PP composites.

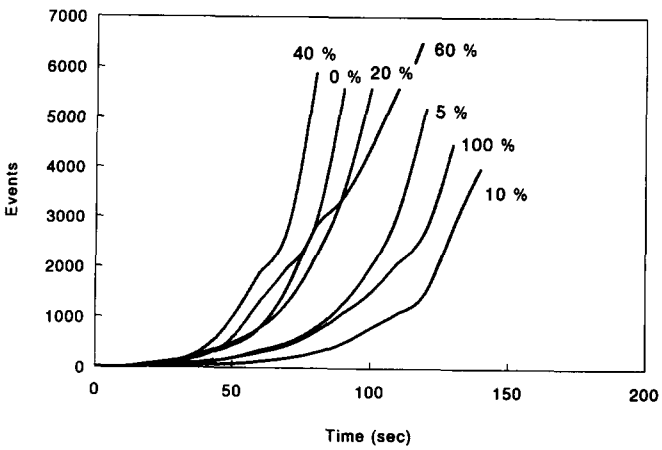


**Fig. 10.** Cumulative AE plots of longitudinally loaded glass/PP composites.

Generally, low-amplitude emissions are associated with low-energy fracture processes such as matrix fracture and/or debonding, whereas fibre fracture is characterized by high-amplitude emissions. Figure 11(a) and (b) shows the distribution of the peak

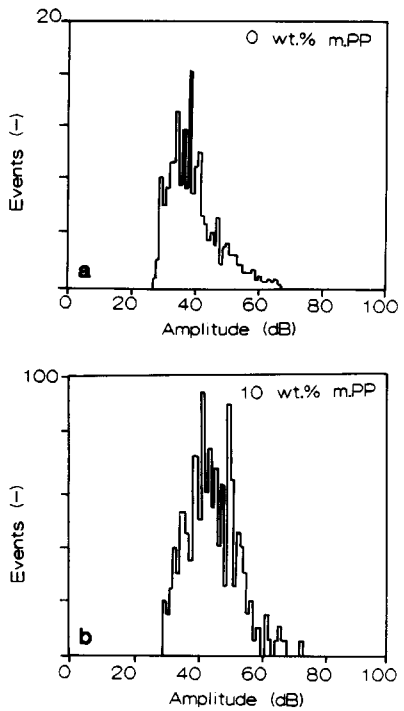


**Fig. 11.** Amplitude distribution of glass/PP composites with 0 wt% and 10 wt% m-PP in the PP matrix.

amplitudes of the AE signals for composites with 0 wt% and 10 wt% m-PP, respectively, loaded to 500 MPa. In composites with 0 wt% m-PP, only low-amplitude signals were registered (Fig. 11(a)), indicative of matrix cracking and/or debonding as the principal failure processes. This can be explained by the poor adhesion between the matrix and the fibre, which prevents effective stress transfer from the matrix to the fibre and thus results in cumulative weakening of the composite by matrix fracture or yielding and debonding. At 10 wt% m-PP the interface is strong enough to sustain higher loads, and stresses can easily be transferred from the matrix to the fibre; this results in more effective loading of the fibre and consequently fibre fracture. Therefore high-amplitude signals also are registered in composites with 10 wt% m-PP (Fig. 11(b)).

Scanning electron micrographs (Fig. 12(a)–(c)) show the fracture surfaces of glass/PP specimens, with 0 wt%, 10 wt% and 100 wt% m-PP in the PP matrix, respectively. The fibres in a composite with 0 wt% m-PP are completely free of matrix material, and the fibres are not held together by the matrix; this finding indicates extensive interfacial failure. In the 100 wt% m-PP composite (Fig. 12(c)), the failure modes are a combination of interface and matrix failure, whereas in the system with 10 wt% m-PP, the fibres are still covered by the polymer matrix; this result indicates matrix failure and relatively good stress transfer. The longitudinal flexural strengths (Fig. 13), and the failure modes of the various glass/PP composites,

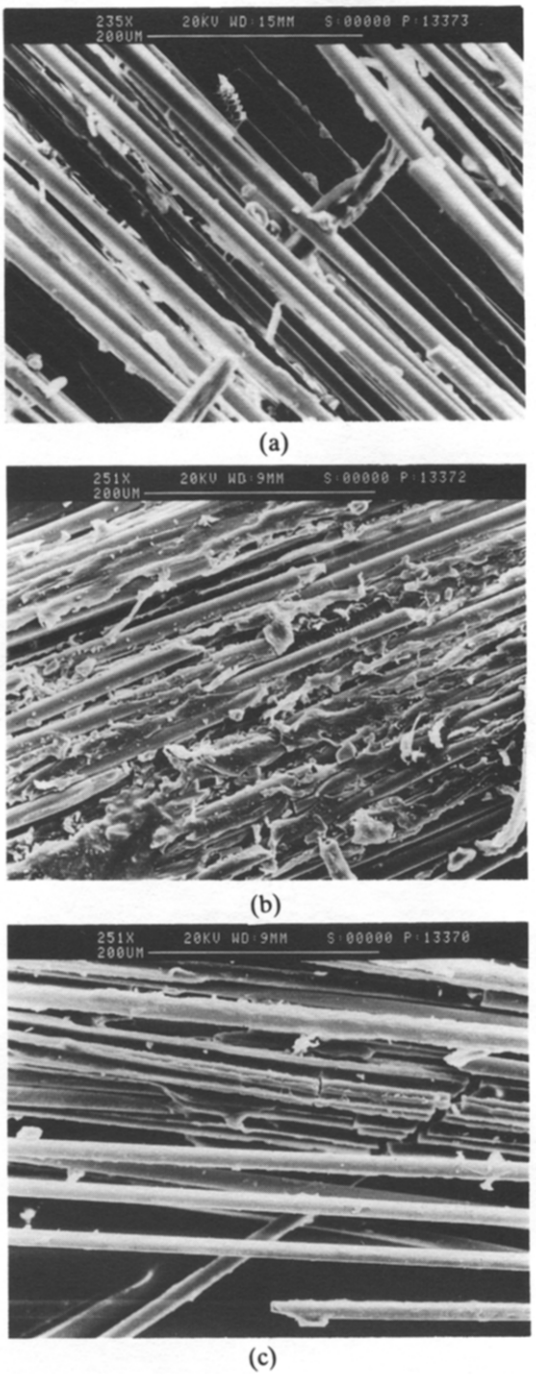


**Fig. 12.** Scanning electron micrograph of longitudinal fracture surfaces showing (a) interface failure at 0 wt% m-PP, (b) matrix failure at 10 wt% m-PP and (c) a combination of interface and matrix failure at 100 wt% m-PP.

show the same trend as those of transversely tested composites.

When comparing the longitudinal flexural moduli of the composites, no significant difference is observed (Fig. 14). Improved adhesion has no significant influence on the longitudinal composite modulus because this composite property is primarily dominated by the modulus of the fibre and its volume fraction.

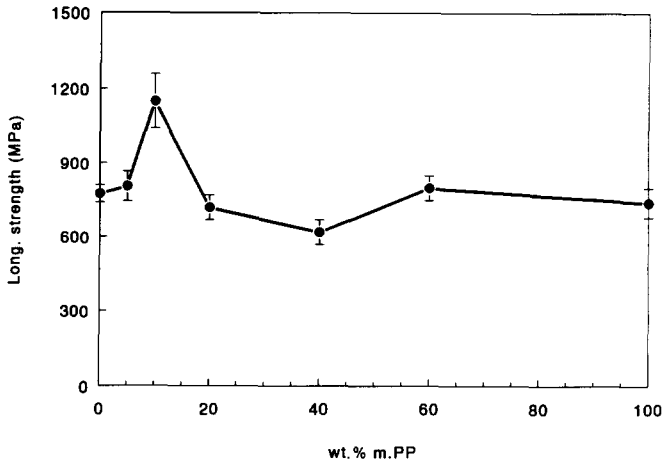


**Fig. 13.** Longitudinal flexural strength of glass/PP composites as a function of the weight fraction of m-PP in the PP matrix.

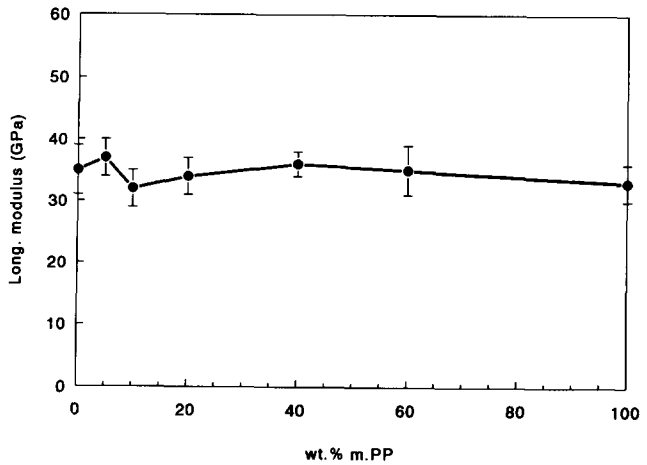


**Fig. 14.** Longitudinal flexural modulus of glass/PP composites as a function of the weight fraction of m-PP in the PP matrix.

### 3.2. Mechanical properties

*3.2.1 Longitudinal tension*

In the previous section, it was shown that for both transverse and longitudinal flexural testing an optimum in strength was observed for composites based on a matrix with 10 wt% m-PP. In the following sections, we will consider some further engineering properties of PP/glass composites, and will focus on two composite systems with 0 wt% and 10 wt% m-PP, which reflect the extremes in interfacial bond strength.

The results of the mechanical tests of the specimens with 0 wt% and 10 wt% m-PP are summarized in Table 3. In this table, a relatively small increase in longitudinal strength and strain is reported, which can be explained by greater effectiveness of the reinforcing fibres, as a result of an increase in fibre/matrix interaction in the composite system with 10 wt% m-PP.

**Table 3. Tensile, shear and compressive properties of UD composites with 0 wt% and 10 wt% m-PP**

| Test | 0 wt% m-PP | 10 wt% m-PP |
|---|---|---|
| *Tension* | | |
| [0], $E_{11}$ (GPa) | 43·4 ± 1·4 | 43·6 ± 2·0 |
| [0], $\sigma_{11}$ (MPa) | 720 ± 50 | 890 ± 60 |
| [0], $\varepsilon_{11}$ (%) | 1·8 ± 0·02 | 2·0 ± 0·01 |
| [90], $E_{22}$ (GPa) | 7·2 ± 2·0 | 5·8 ± 0·6 |
| [90], $\sigma_{22}$ (MPa) | 4·2 ± 2·0 | 9·7 ± 1·5 |
| [90], $\varepsilon_{22}$ (%) | 0·05 ± 0·02 | 0·14 ± 0·02 |
| *Shear* | | |
| [10], $\tau_{12}$ (MPa) | 11·4 ± 3·0 | 17·0 ± 1·0 |
| [±45], $\tau_{12}$ (MPa) | 9·6 ± 0·8 | 13·6 ± 1·0 |
| SBS, $\tau_{13}$ (MPa) | 16·0 ± 0·3 | 21·0 ± 0·4 |
| *Compression* | | |
| [0], $\sigma_{11c}$ (MPa) | 250 ± 70 | 396 ± 40 |
| [90], $\sigma_{22c}$ (MPa) | 35·7 ± 1·5 | 37·5 ± 1·5 |

Based on a rule of mixture relationship for the tensile strength of fibre-reinforced composites, including an effectivity parameter $k$, the influence of m.PP on the fibre efficiency can be demonstrated:

$$\sigma_c = k[\sigma_f V_f + E_m \varepsilon_f (1 - V_f)] \quad (6)$$

where $\sigma_c$ is the composite tensile strength, $\sigma_f$ is the fibre tensile strength, $E_m$ is the stiffness of the matrix, $\varepsilon_f$ is the failure strain of the fibre and $V_f$ is the fibre volume fraction. A typical value for the tensile strength of $E$-glass fibres as obtained from impregnated strand tests is approximately 2400 MPa. Using the matrix moduli as listed in Table 1, a fibre failure strain of 0·033 and a fibre volume fraction of 0·58, the effectivity parameter $k$ yields values of 0·51 and 0·63 for composites with 0 wt% and 10 wt% m-PP, respectively. However, even in the case of a 10 wt% m-PP composite system, fibre efficiency is rather low in comparison with that of glass-fibre-reinforced systems based on epoxy resins, and yields values for $k$ in the order of 0·85–0·95.

Comparison between the tensile and flexural test results of the two composite systems showed that the longitudinal flexural strengths are a little higher than the longitudinal tensile strengths (8% and 17% increase for 0 wt% and 10 wt% m-PP composites, respectively). Differences can be explained by differences in critically loaded volume, i.e. size effects. In a three-point bend test only the outer fibres at the mid-span of the beam are loaded up to their maximum stress, whereas in tension the whole composite volume is critically loaded, yielding a higher probability of failure.

Similar to flexural testing, the longitudinal tensile modulus remained constant and is in good agreement with theoretical predictions based on a rule of

mixtures relationship:

$$E_c = E_f V_f + E_m(1 - V_f) \quad (7)$$

where $E_c$ and $E_f$ are the tensile moduli of the composite and fibre, respectively. Using a fibre tensile modulus of 73 GPa, eqn (7) yields a theoretical composite modulus of 44·4 GPa. This predicted value falls within the experimental scatter of the values as listed in Table 3, indicating that the quality of the unidirectional composites with respect to such factors as fibre straightness and inhomogeneities is rather good.

*3.2.2 Transverse tension*

The transverse strength and strain increased by 130% and 180%, respectively, as a result of addition of m-PP. As off-axis composite properties such as transverse strength and strain are strongly dominated by the interface, an increase in interaction between matrix and fibre as a result of the addition of m-PP resulted in a remarkable increase in transverse properties. A large difference is seen when comparing the transverse flexural strengths with the transverse tensile strengths; this indicates large size effects and a high sensitivity to small imperfections at the surface of the specimen. In transversely loaded composites in particular, where fibre, matrix and interface are acting in series and strength is often governed by the strength of the weakest link, relatively large size effects can occur.

Semi-crystalline materials such as PP behaves in a rather elastic manner after crystallization at low cooling rates (1°C $min^{-1}$) and high pressures.[28,29] In the glass/PP composite, glass fibres act as nucleation points for crystallization of PP. The high volume fraction of glass fibres results in significant interaction between growing crystals. This combination of low cooling rate, high pressure and interactions between growing crystals might result in a brittle and notch-sensitive PP matrix and consequently the low strain to failure of the glass/PP composite.

*3.2.3 Shear*

As shown in Table 3, an increase in in-plane shear strength as calculated from the 10° off-axis and ±45° tensile tests was also observed. Addition of 10 wt% m-PP resulted in an increase in in-plane (1–2) shear strength of 49% and 42% for the 10° off-axis and ±45° tensile tests, respectively. The $[\pm 45]_{4s}$ cross-ply laminates were manufactured from 0·3 mm thick prepregs which were moulded in a similar manner to the unidirectional composites. However, for these prepregs only one layer of fibre was applied. Short beam shear tests yielded the highest values for the composite shear strength: 16 MPa and 21 MPa for 0 wt% and 10 wt% m-PP composites, respectively. However, addition of 10 wt% m-PP resulted in only a 30% increase in interlaminar (1–3) shear strength, which is significantly lower than the increase in in-plane shear strength as obtained from the off-axis tensile tests. Similar findings were reported by Madhukar and Drzal,[12] who investigated the shear properties of carbon fibre/epoxy composites using different shear tests. They also found that the shear strength of carbon fibre composites incorporating carbon fibres with different surface treatments, as measured by the short beam shear test, increased at a lower rate with adhesion level than the shear strength as measured by ±45° tension tests. Differences were attributed to 'scissoring' effects in the ±45° tension test in the case of composites with poor adhesion between fibre and matrix.

The typical stress/strain curves for both types of ±45 laminates shown in Fig. 15 reveal the non-linear response in tension. In particular, in the case of 0 wt% m-PP composites, this non-linearity leads to high failure strains, of the order of 25–30%. The failure strain of 0 wt% m-PP composites with poor levels of adhesion was much higher than that of the 10 wt% m-PP composite, as a result of a more brittle failure process of the latter (Fig. 16). Although the initial modulus is the same for both types of laminate, there is an increase in stress at which irreversible deformation starts to occur. Remarkably, the maximum failure stress for the 0 wt% m-PP composites was higher than that for composites with m-PP. Because of the poor adhesion in the 0 wt% m-PP composite, delamination between the individual plies manifests itself at low loads, and results in a rotation of the fibres in the loading direction from ±45° to ±34°. In composites with improved fibre/matrix adhesion, only little interply failure occurs; therefore, extensive fibre rotation (±43°) is prevented and the failure process is more local. As

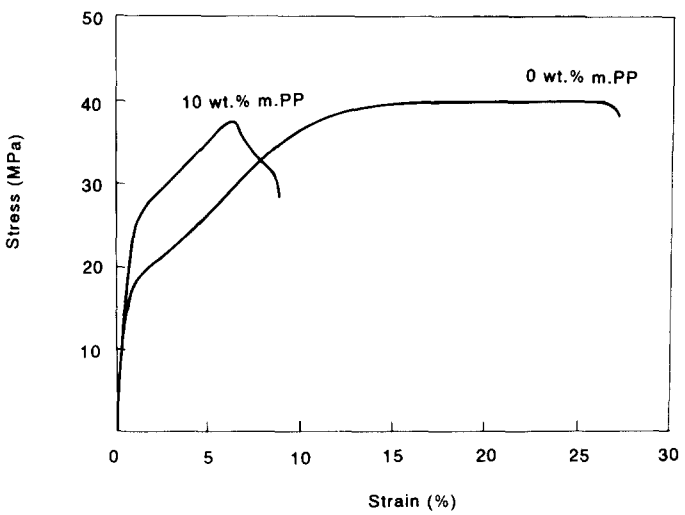


**Fig. 15.** Stress/strain curves for $[\pm 45]_{4s}$ PP/glass laminates in tension.

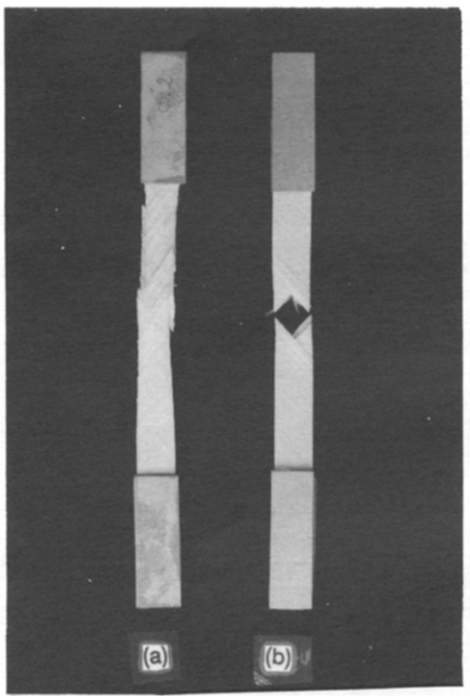


**Fig. 16.** Photographs of failed ±45 tension specimens showing (a) extensive matrix cracking and delamination throughout the entire 0 wt% m-PP composite and (b) more local failure processes for the 10 wt% m-PP composite.

these 'scissoring' effects lead to false readings, the in-plane shear strength as listed in Table 3 was calculated from eqn (5), by using the stress at the first knee in the stress/strain curve.

*3.2.4 Compression*

In contrast to the tensile strength, the compression strength of composite materials is sensitive to the properties of the matrix and the interface.[11,14] For a thermoplastic composite system based on carbon fibre/PEEK a compression strength about 30% lower than that of equivalent epoxy composites was reported.[33] As the resistance to fibre buckling is provided by the shear modulus of the matrix, this deterioriation in properties can be related to the relatively low shear moduli and yield strengths of linear polymers in comparison with highly crosslinked systems.

The compression test results are summarized in Table 3; they show an approximate 60% increase in longitudinal compressive strength for the 10 wt% m-PP composite. A combination of longitudinal splitting and fibre buckling as the predominant failure modes was observed for all specimens tested. The occurrence of matrix- and interface-dominated failure modes rather than fibre-dominated failure modes yielded relatively low values for the compression strength of PP/glass composite in comparison with data for glass-fibre-reinforced epoxies.

Although the transverse compression strength is an interface-dominated composite property with typical 45° shear failure modes, almost no effect of the addition of m-PP on this property was observed.

## 4 CONCLUSIONS

This study showed an increase in composite strength as a result of the addition of maleic-anhydride-modified PP to continuous-glass-fibre-reinforced PP composites. An optimum in both longitudinal and transverse flexural strength was reached for composites based on a PP matrix with 10 wt% m-PP. Scanning electron micrographs showed a change in failure mode from debonding to matrix fracture for 10 wt% m-PP composites, indicating an optimum in adhesion between the matrix and the fibre for this composite system. At higher weight fractions of m-PP a decrease in flexural strength was observed, and fractographs showed a change to more interfacial dominated failure modes.

These results indicate that, in addition to the adhesion level between the matrix and the fibre, the interphase and/or matrix properties were also influenced by the addition of m-PP to the glass/PP composite, which caused a decrease in strength at higher weight fractions of m-PP.

Additional tensile, shear and compression tests on unidirectional glass/PP composites with 0 wt% and 10 wt% m-PP showed that improved adhesion as a result of the addition of m-PP had little influence on the composite moduli. A small increase in longitudinal tensile strength and strain was observed for 10 wt% m-PP composites, whereas off-axis composite properties that are governed by the interphase, such as transverse, shear and compression strength, showed a relatively large increase.

## REFERENCES

1. Harper, R. C., Thermoforming of thermoplastic matrix composites, Part I. *SAMPE J.*, **28**(2) (1992) 9.
2. Harper, R. C., Thermoforming of thermoplastic matrix composites, Part II. *SAMPE J.*, **28**(3) (1992) 9.
3. Cogswell, F. N., *Thermoplastic Aromatic Polymer Composites*. Butterworth–Heinemann, Oxford, 1992.
4. Bigg, D. M. & Preston, J. R., Stamping of thermoplastic matrix composites. *Polymer Composites*, **10**(4) (1989) 26.
5. Lowe, A. C., Moore, D. R. & Robinson, I. M., Data for designing with continuous glass fibre reinforced polypropylene. In *Proc. 5th European Conference on Composite Materials*, ed. J. Fuller, G. Gruninger, K. Schulte, A. R. Bunsell & A. Massiah. Elsevier Applied Science, Publishers, Barking, UK, 1990, p. 1073.
6. Marissen, R., Hornman, H. H. H., Wenmakers, L. E. P. & Scholle, K. F. M. G. J., Advanced thermoplastic composites for low cost structural applications. In *Proc. 11th Int. European Chapter Conf. of SAMPE*, ed. H. L. Hornfeld, SAMPE European Chapter, Basel, 1990, p. 41.
7. Talbott, M. F., Springer, G. S. & Berglund, L. A., The effects of crystallinity on the mechanical properties of

PEEK polymer and graphite fiber reinforced PEEK. *J. Composite Mater.*, **21** (1987) 1056.
8. Ye, L. & Friedrich, K., Relationships between microstructure and interlaminar fracture toughness of commingled yarn based glass/polypropylene composites. In *Proc. 6th European Conference on Composite Materials*, ed. A. R. Bunsell, J. F. Jamet & A. Massiah, European Association for Composite Materials, Bordeaux, 1992, p. 261.
9. Ishida, H. (ed.), *Controlled Interphases in Composites Materials*. Elsevier, New York, 1990.
10. Verpoest, I. & Jones, F. (eds.), *Interfacial Phenomena in Composite Materials '91*. Butterworth–Heinemann, Oxford, 1991.
11. Norita, T., Matsui, J. & Matsuda, H. S., *Proc. 2nd Int. Conf. on Composite Interfaces*, ed. H. Ishida & J. L. Koenig. Elsevier Applied Science Publishers, Cleveland, 1986, p. 123.
12. Madhukar, M. S. & Drzal, L. T., Fiber–matrix adhesion and its effect on composite mechanical properties: I Inplane and interlaminar shear behaviour of graphite/epoxy composites. *J. Composite Mater.*, **25** (1991) 932.
13. Madhukar, M. S. & Drzal, L. T., Fiber–matrix adhesion and its effect on composite mechanical properties: II. Longitudinal (0°) and transverse (90°) tensile and flexure behaviour of graphite/epoxy composites. *J. Composite Mater.*, **25** (1991) 958.
14. Madhukar, M. S. & Drzal, L. T., Fiber–matrix adhesion and its effect on composite mechanical properties: III. Longitudinal (0°) compressive properties of graphite/epoxy composites. *J. Composite Mater.*, **26** (1992) 310.
15. Ivens, J., Wevers, M. & Verpoest, I., Influence of carbon fibre surface treatment on the mode I fracture toughness in CRFP. In *Proc. 8th Int. Conf. Composite Material*, ed. S. W. Tsai & G. S. Springer. SAMPE, Honolulu, 1991, 11C.
16. Shih, G. C. & Ebert, L. J., Effect of interface on fatigue performance of unidirectional fiber glass composites. *Composites Sci. Technol.*, **28** (1987) 137.
17. Peijs, A. A. J. M. & de Kok, J. M. M., Hybrid composites based on polyethylene and carbon fibres. Part 6: tensile and fatigue behaviour. *Composites*, **24** (1993) 19.
18. Ishida, H., A review of recent progress in studies of molecular and microstructure of coupling agents and their functions in composites, coatings and adhesive joints. *Polymer Composites*, **5** (1984) 101.
19. Plueddemann, E. P., *Silane Coupling Agent*. Plenum, New York, 1982.
20. Mäder, E. & Freitag, K., Interface properties and their influence on short fibre composites. *Composites*, **21** (1990) 397.
21. Xanthos, M., Interfacial agents for multiphase polymer systems: recent advances. *Polymer Eng. Sci.*, **28** (1988) 1392.
22. Constable, A. R. C. & Humenik, J. A., Performance enhancement in glass fibre reinforced polypropylene obtained by the addition of acrylic acid grafted polypropylene. In *SPI 44th Annual Reinforced Plastics/Composites Institute Conference*, Anaheim, 1989, p. 11A.
23. Daemen, J. M. H. & den Besten, J., The influence of glass fibre sizing on the properties of GF/PP. *Eng. Plastics*, **4**(2) (1991) 82.
24. Moore, D. R., Fatigue of thermoplastic composites. In *Thermoplastic Composite Materials* (*Composite Materials Series*: *7*), ed. L. A. Carlsson. Elsevier Science Publishers, Barking, 1991, p. 331.
25. Silverman, E. & Jones, R. J., Properties and processing of graphite/PEEK prepreg tapes and fabrics. *SAMPE J.*, **24**(4) (1988) 33.
26. Lee, W. I. & Springer, G. S., A model of the manufacturing processs of themoplastic matrix composites. *J. Composite Mater.*, **21** (1987) 1017.
27. Evans, R. E. & Masters, J. E., New generation of composites for structural applications: materials and mechanics. In *Toughened Composites, ASTM STP 937*, ed. N. J. Johnston. American Society for Testing and Materials, Philadelphia, PA, p. 74.
28. Barish, L., *J. Appl. Polymer Sci.*, **6** (1962) 617.
29. Mears, D. R., Pae, K. D. & Sauer, J. A., *J. Appl. Phys.*, **40** (1969) 4229.
30. Folkes, M. J. & Hardwick, S. T., The mechanical properties of glass/polypropylene multilayer laminates. *J. Mater. Sci.*, **25** (1990) 2598.
31. Davies, P. & Echalier, B., The fibre–matrix interface region in stampable glass fibre polypropylene composites. *J. Mater. Sci. Lett.*, **8** (1989) 1241.
32. Berthelot, J. M., Relation between amplitudes and rupture mechanisms in composite materials. *J. Reinf. Plast. Composites*, **7** (1988) 284.
33. Leeser, D. & Leach, D. C., Compressive properties of thermoplastic matrix composites. In *34th Int. SAMPE Symp.*, SAMPE, Anaheim, 1989, p. 1464.